JOURNAL OF MATERIALS SCIENCE 39 (2004) 3309–3318

# Synthesis of HDLC films from solid carbon

R. L. MILLS, J. SANKAR, P. RAY, A. VOIGT, J. HE, B. DHANDAPANI
*BlackLight Power, Inc., 493 Old Trenton Road, Cranbury, NJ 08512, USA*
*E-mail: rmills@blacklightpower.com*

Diamond-like carbon (DLC) films were synthesized on silicon substrates from solid carbon by a very low power (~60 W) microwave plasma chemical vapor deposition (MPCVD) reaction of a mixture of 90–70% helium and 10–30% hydrogen. It is proposed that $He^+$ served as a catalyst with atomic hydrogen to form an energetic plasma. The average hydrogen atom temperature of a helium-hydrogen plasma was measured to be up to 180–210 eV versus ≈3 eV for pure hydrogen. Bombardment of the carbon surface by highly energetic hydrogen formed by the catalysis reaction may play a role in the formation of DLC. The films were characterized by time of flight secondary ion mass spectroscopy (ToF-SIMS), X-ray photoelectron spectroscopy (XPS), and Raman spectroscopy. TOF-SIMS identified the coatings as hydride by the large $H^+$ peak in the positive spectrum and the dominant $H^-$ in the negative spectrum. The XPS identification of the H content of the CH coatings as a novel hydride corresponding to a peak at 49 eV has implications that the mechanism of the DLC formation may also involve one or both of selective etching of graphitic carbon and the stabilization of $sp^3$-bonded carbon by the hydrogen catalysis product. Thus, a novel H intermediate formed by the plasma catalysis reaction may enhance the stabilization and etching role of H used in past methods. © *2004 Kluwer Academic Publishers*

## 1. Introduction

Diamond-like carbon (DLC) has unique material properties and may be coated on an array of materials such as metallic, ceramic, and optical materials. Its extremely high hardness, high chemical inertness, low friction coefficient, high ductility, wear resistance, relatively high thermal conductivity, and high transparency across a large part of the electromagnetic spectrum makes DLC suitable for many applications such as wear protective or resistant coatings for mechanical tools, infrared optics, and sensors designed to work in corrosive environments. They may be used as protective coatings for hip replacements and other medical implants due to their biocompatibility. Further applications include corrosion protection, liquid and vapor transport barriers, electronic devices, and electron field emitting cathode materials. Characteristics which makes them good candidates for inter-metal dielectrics in integrated circuits are that they are good insulators and have a high breakdown voltage. Recently, DLC film has been applied in large-area flat panel displays due to their field-emission properties [1–7].

DLC or tetrahedral amorphous carbon (Ta-C) consists mainly of $sp^3$ bonded carbon atoms. If properly prepared, DLC can have properties that rival those of crystalline diamond. The beneficial properties of DLC stem from the continuous rigid random networks of $sp^3$ carbon atoms, and the properties can essentially be tailored by controlling the $sp^3/sp^2$ ratio. The mechanism of low-temperature ion sputter deposition involves energetic ion bombardment during the deposition of carbon which leads to the formation of diamond-like amorphous carbon. In the absence of ion bombardment during deposition, soft, conductive carbon films form with no diamond-like properties. A selective ion energy range is necessary. Films with more pronounced diamond-like properties are produced at low ion energies (less than 100 eV), and microcrystalline diamond growth characteristic of DLC films decreases with increasing ion energy (more than 100 eV) [8–10]. Ultimately amorphous carbon deposition occurs with excessive ion energy. Prawer *et al.* [11] using a mass selected $C^+$ ion beam deposition system showed that the $sp^2$ content of films decreased as the ion energy is increased from about 10 to 300 eV, and for films made with ion energies in excess of 1 keV, the $sp^2$ content increased with increasing ion energy. In a DLC review article, Wei and Narayan [12] discuss the mechanism of DLC formation by ion bombardment wherein energetic ions cause lateral carbon atom motion to advantageous sites, sputter impurity gases from the surface, and preferentially remove less stable carbon such as $sp^2$-bonded carbon.

The incorporation of hydrogen is believed to stabilize DLC films. Based on experience of CVD processing with hydrocarbons, it was thought by many authors that the presence of hydrogen was a necessary condition for the formation of DLC [12]. Correlations between $sp^3$ fraction and hydrogen content were developed. But, the essential role of hydrogen was eliminated by the discovery of the formation of high quality DLC films by pulsed laser ablation of pure carbon that provides an alternative

mechanism. The mechanism of PLD which clearly shows that the presence of hydrogen is not necessary for the formation of $sp^3$ bonds, is very different from the hot-ion bombardment mechanism. In PLD, highly energetic photons from pulsed laser beams excite $sp^2$ bonded carbon atoms into a C* (excited carbon) state, and these excited carbon atoms subsequently cluster to form DLC according to the following reactions [12]:

$$C(sp^2\,\text{bonded}) + h\nu \rightarrow C^* \quad (1)$$

$$C^* + C^* \rightarrow (sp^3\,\text{bonded}) \quad (2)$$

Therefore, the DLC synthesis and processing methods of hydrogenated (a-C:H) or hydrogen-free (a-C) films may be divided into two groups of low pressure techniques: chemical vapor deposition (CVD) and physical vapor deposition (PVD) methods involving carbon bearing compounds; and PVD methods based on energetic ablation of carbon. The first group includes ion assisted CVD deposition or ion beam-assisted deposition (IBAD) using ionized hydrocarbon gases [13, 14], plasma enhanced deposition using a DC glow discharge from hydrocarbon gas [15], radio-frequency (RF) discharged plasma enhanced chemical vapor deposition (PE-CVD) using a hydrocarbon gas [16, 17], microwave discharge [18], electron cyclotron resonance (ECR) discharge [19], and so on. The second includes filtered cathodic vacuum arc deposition (FC-VAD) [20–22], sputtering of carbon targets (graphite) [23], mass selected ion beam deposition (MS-IBD) [24], pulsed laser ablation (PLA) [25], and so forth.

In a quest to extend the techniques to form DLC with the possibility of using very low power levels, we explored the possibility of using unique plasmas which are very energetic and form very stable hydrides wherein both of these features may cause the formation of DLC. The most common method of forming DLC films uses the acceleration of charged particles by high biased field or by using high power RF or microwaves to produce fast ions of about 100 eV for bombarding depositing graphitic carbon film to force conversion to DLC. Mills *et al.* [26] have shown that it is possible to form fast H in certain plasmas by a nonfield-acceleration mechanism. From the width of the 656.3 nm Balmer $\alpha$ line emitted from microwave and glow discharge plasmas, it was found that a strontium-hydrogen microwave plasma showed a broadening similar to that observed in the glow discharge cell of 27–33 eV; whereas, in both sources, no broadening was observed for magnesium-hydrogen. Microwave helium-hydrogen and argon-hydrogen plasmas showed extraordinary broadening corresponding to an average hydrogen atom temperature of 180–210 eV and 110–130 eV, respectively. The corresponding results from the glow discharge plasmas were 33–38 eV and 30–35 eV, respectively, compared to ≈3 eV for plasmas of pure hydrogen, neon-hydrogen, krypton-hydrogen, and xenon-hydrogen maintained in either source. External Stark broadening or acceleration of charged species due to high fields can not explain the microwave results since no high field was present, and the electron density was orders of magnitude too low for the corresponding Stark effect. Rather, a proposed resonant energy transfer mechanism explains these results [26]. In the case of helium-mixed plasmas, $He^+$ serves as a catalyst to resonantly accept energy equivalent to two times the potential energy of atomic hydrogen, $E_h = 27.2$ eV where $E_h$ is one Hartree. The theory has been given previously [27, 28].

Furthermore, it was previously reported that a novel highly stable surface coating SiH($1/p$) which comprised high binding energy hydride ions was synthesized by microwave plasma reaction of mixture of silane, hydrogen, and helium wherein it was proposed that $He^+$ served as a catalyst with atomic hydrogen to form the highly stable hydride ions [29]. Novel silicon hydride was identified by time of flight secondary ion mass spectroscopy and X-ray photoelectron spectroscopy. The time of flight secondary ion mass spectroscopy (ToF-SIMS) identified the coatings as hydride by the large $SiH^+$ peak in the positive spectrum and the dominant $H^-$ in the negative spectrum. X-ray photoelectron spectroscopy (XPS) identified the H content of the SiH coatings as hydride ions, $H^-$ (1/4), $H^-$ (1/9), and $H^-$ (1/11) corresponding to peaks at 11, 43, and 55 eV, respectively. The silicon hydride surface was remarkably stable in air for long duration exposure as shown by XPS.

Solid glassy or graphitic carbon was used as the carbon source in the helium-hydrogen microwave plasma having documented fast H [26] which causes DLC to form. These plasmas also form novel hydrides which may stabilize $sp^3$ carbon. We report the deposition of DLC on silicon-wafers from a solid carbon precursor and a helium-hydrogen (90–70/10–30%) microwave plasma maintained with an Evenson cavity under low power (~60 W), mild conditions. After the plasma processing reaction, the surface was characterized by ToF-SIMS, XPS, and Raman spectroscopy. ToF-SIMS and XPS provided means to assess the role of any hydrides. In order to understand the role of the helium-hydrogen plasma, it was characterized by recording the line broadening of the 656.3 nm Balmer $\alpha$ line to determine the excited hydrogen atom kinetic energy.

## 2. Experimental

### 2.1. Synthesis

H*DLC films were grown on silicon wafer substrates by their exposure to a low pressure $He/H_2$ microwave plasma with 0.1 g of solid glassy carbon foil (5 × 5 × 1 mm, Alpha Aesar 99.99%) or graphite foil (10 × 10 × 1 mm, Alpha Aesar 99.99%). The experimental set up comprising a microwave discharge cell operated under flow conditions is shown in Fig. 1. The carbon source was placed in the center of the microwave cavity, and a silicon wafer substrate (5 × 5 × 0.05 mm, Alfa Aesar 99+%) cleaned by heating to 700°C under vacuum was placed about 20 mm off center inside of a quartz tube (12 mm in diameter by 0.25 m long) with vacuum valves at both ends. The tube was center-fitted with an Opthos coaxial microwave cavity (Evenson cavity) and connected to the gas/vacuum line. The quartz tube and vacuum line were evacuated for 2 h to remove any trace moisture or oxygen and residual

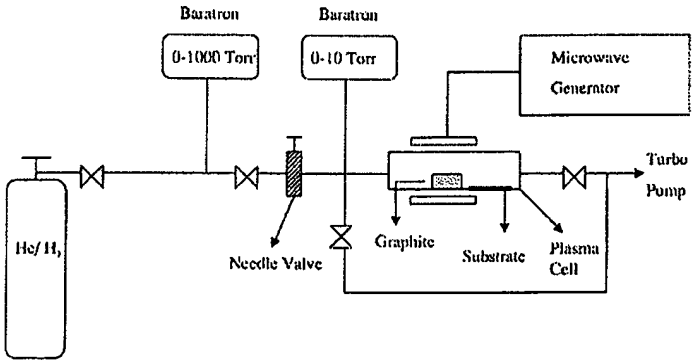


*Figure 1* The experimental set up comprising a microwave discharge cell operated under flow conditions.

gases. A premixed He (90–70%)/$H_2$ (10–30%) plasma gas was flowed through the quartz tube at a total pressure of $2 \times 10^2$ N/m$^2$ maintained with a gas flow rate of 40 sccm controlled by a mass flow controller with a readout. The cell pressure was monitored by an absolute pressure gauge. The microwave generator shown in Fig. 1 was an Opthos model MPG-4M generator (Frequency: 2450 MHz). The microwave plasma was maintained with a 65 W (forward)/4 W (reflected) power for about 12–16 h. The carbon source was located in the center of the plasma, and the substrate was at the cool edge of the plasma glow region. The wall temperature at this position was about 300°C. A thick (~100 $\mu$m translucent, golden-yellow, shiny coating formed on the substrate and the wall of the quartz reactor. The quartz tube was removed and transferred to a drybox with the samples inside by closing the vacuum valves at both ends and detaching the tube from the vacuum/gas line. The coating on the inside of the wall of the reactor tube was collected by etching the tube for 5–10 min with 1% dilute hydrofluoric acid. The coating was then detached from the surface and peeled off as a 30 mm long unsupported transparent thin film. The coated silicon wafer substrate was mounted on XPS and ToF-SIMS sample holders under an argon atmosphere in order to prepare samples for the corresponding analyses. Controls for XPS analysis comprised a cleaned commercial silicon wafer (Alfa Aesar 99.99%) and known standards: (a) single crystal diamond, (b) diamond film, (c) glassy carbon, (d) pyrolytic graphite, (e) mineral graphite, and (f) HDLC (hydrogenated diamond-like carbon). The control for ToF-SIMS analysis comprised a cleaned commercial silicon wafer (Alfa Aesar 99.99%). The coated substrate and thin film were also sent for Raman analysis (Charles Evans & Associates, Sunnyvale, CA).

## 2.2. ToF-SIMS characterization

Cleaned commercial silicon wafers before and after plasma treatment to form a H*DLC film coating were characterized using a Physical Electronics TRIFT ToF-SIMS instrument. The primary ion source was a pulsed $^{69}Ga^+$ liquid metal source operated at 15 keV. The secondary ions were extracted by a ±3 keV bias (according to the mode) voltage. Three electrostatic analyzers (Triple-Focusing-Time-of-Flight) deflect them in order to compensate for the initial energy dispersion of ions of the same mass. The 400 pA dc current was pulsed at a 5 kHz repetition rate with a 7 ns pulse width. The analyzed area was 60 $\mu$m × 60 $\mu$m and the mass range was 0–1000 AMU. The total ion dose was $7 \times 10^9$ ions/mm$^2$, ensuring static conditions. Charge compensation was performed with a pulsed electron gun operated at 20 eV electron energy. In order to remove surface contaminants and expose a fresh surface for analysis, the samples were sputter-cleaned for 30 s using a 80 $\mu$m × 80 $\mu$m raster, with 600 pA current, resulting in a total ion dose of $10^{13}$ ions/mm$^2$. Three different regions on each sample of 60 $\mu$m × 60 $\mu$m were analyzed. The positive and negative SIMS spectra were acquired. Representative post sputtering data is reported. The ToF-SIMS data were treated using 'Cadence' software (Physical Electronics), which calculates the mass calibration from well-defined reference peaks.

## 2.3. XPS characterization

A series of XPS analyses were made on the samples using a Scienta 300 XPS Spectrometer at Lehigh University, Bethlehem, PA. The fixed analyzer transmission mode and the sweep acquisition mode were used. The Al X-ray incidence angle was 15°. The step energy in the survey scan was 0.5 eV, and the step energy in the high resolution scan was 0.15 eV. In the survey scan, the time per step was 0.4 s, and the number of sweeps was 4. In the high resolution scan, the time per step was 0.3 s, and the number of sweeps was 30. C1*s* at 284.6 eV was used as the internal standard.

## 2.4. Raman spectroscopy

Experimental and control samples were analyzed by Charles Evans & Associates, Sunnyvale, CA. Raman spectra were obtained with a LABRAM spectrometer (Dilor of Jobin Yvon) with a Spectrum One CCD (charge coupled device) detector (Spex and Jobin Yvon) that was air and Peltier cooled. An Omnichrome HeNe laser (Melles Griot) with the light wavelength of 632.817 nm was used as the excitation source. The spectra were taken at ambient conditions and the samples were placed under a Raman microscope (Olympus BX40). Spectra of the film samples were acquired using the following condition: the laser power at the sample

was 4 to 8 mW, the slit width of the monochromator was 100 $\mu$m which corresponds to a resolution of 3 $cm^{-1}$, the detector exposure time was 20 min, and 3 scans were averaged.

### 2.5. Visible spectroscopy and Balmer line broadening measurements

The width of the 656.3 nm Balmer $\alpha$ line from hydrogen alone, xenon-hydrogen mixture (90/10%), and helium-hydrogen mixture (90/10%) microwave discharge plasmas maintained in the microwave discharge cell shown in Fig. 1 was measured with a high resolution visible spectrometer capable of a resolution of ±0.006 nm according to methods given previously [26]. The spectra were recorded over the region 656.0–657.0 nm. The 667.816 nm He I line width was also recorded with the high resolution (±0.006 nm) visible spectrometer on helium-hydrogen (90/10%) and helium microwave discharge plasmas.

To measure the absolute intensity, the high resolution visible spectrometer and detection system were calibrated [30] with 546.08, 576.96, and 696.54 nm light from a Hg-Ar lamp (Ocean Optics, model HG-1) that was calibrated with a NIST certified silicon photodiode. The population density of the $n = 3$ hydrogen excited state $N_3$ was determined from the absolute intensity of the Balmer $\alpha$ (656.3 nm) line measured using the calibrated spectrometer. The spectrometer response was determined to be approximately flat in the 400–700 nm region by ion etching and with a tungsten intensity calibrated lamp.

The electron density was determined using a Langmuir probe according to the method given previously [31].

## 3. Results

### 3.1. ToF-SIMS

The positive ion ToF-SIMS spectra ($m/e$ = 0–200) of a cleaned commercial silicon wafer before and after being coated with a hydrogenated carbon film are shown in Fig. 2a and b, respectively. The positive ion spectrum of the control was dominated by $Si^+$, oxides $Si_xO_y^+$, and hydroxides $Si_x(OH)_y^+$; whereas, that of the hydrogenated carbon film sample contained no silicon containing fragments. Rather, a large $H^+$ peak and hydrocarbon fragments $C_xH_y^+$ were observed as given in Table I.

The negative ion ToF-SIMS spectrum ($m/e$ = 0–200) of a cleaned commercial silicon wafer before and after being coated with a hydrogenated carbon film are shown in Fig. 2c and d, respectively. The control spectrum was dominated by oxide ($O^-$) and hydroxide ($OH^-$); whereas, spectrum of the hydrogenated carbon film was dominated by hydride ion ($H^-$) and carbon ion ($C^-$). Very little oxide ($O^-$) or hydroxide ($OH^-$) was observed.

### 3.2. XPS

A survey spectrum was obtained over the region $E_b = 0$ to 1200 eV. The primary element peaks allowed for the determination of all of the elements present. The XPS survey scan of a cleaned commercial silicon wafer before and after being coated with a hydrogenated carbon film are shown in Figs 3 and 4, respectively. The major peaks identified in the XPS spectrum of the control sample were O1$s$ at 530.6 eV, trace C1$s$ at 284.6 eV, dominant Si 2$s$ at 152.4 eV and Si 2$p_{3/2}$ at 101.9 eV. Whereas, the hydrogenated carbon film sample comprised only carbon and trace silicon and oxygen contamination from the substrate as indicated by the trace O 1$s$ peak at 532.9 eV, the trace Si 2$s$ at 153.2 eV and Si 2$p_{3/2}$ at 102.2 eV, and the dominant C1$s$ peak at 284.6 eV.

The high resolution XPS spectra (0–35 eV) of the valence band region of (a) single crystal diamond, (b) diamond film, (c) glassy carbon, (d) pyrolytic graphite, (e) mineral graphite, and (f) HDLC are shown in Fig. 5 [32]. The corresponding XPS spectrum of the hydrogenated carbon film sample is shown in Fig. 6. The film had a broad peak at 16 eV which matched the peak energy of HDLC rather than that of the other forms of carbon which were observed at higher binding energies. An O2$s$ peak was also observed at 23 eV as shown in Fig. 6.

The high resolution XPS spectra (280–340 eV) of the C1$s$ energy loss region of (a) single crystal diamond, (b) diamond film, (c) glassy carbon, (d) pyrolytic graphite, (e) mineral graphite, and (f) HDLC are shown in Fig. 7 [32]. The corresponding XPS spectrum of the hydrogenated carbon film sample is shown in Fig. 8. Single crystal diamond, diamond film, and HDLC have an energy loss feature which begins at about 290 eV which is at a higher energy than that of the other possible forms of carbon as shown in Fig. 7. The closest match to the shape of the energy loss feature of the carbon film is HDLC to which the film was assigned.

The 0–100 eV binding energy region of high resolution XPS spectra of a cleaned commercial silicon wafer

TABLE I Positive ToF-SIMS fragments of the hydrogenated carbon film formed on a silicon substrate from a helium-hydrogen (95/10%) microwave plasma with the glassy carbon as the souce of C. The mass was calibrated by H (1.0078) and $C_2H_3$ (27.0235)

| M/Z | Fragment/Ion (+) (Count integral > 500) | M/Z | Fragment/ion (+) (200 < Count integral < 500 |
|---|---|---|---|
| 1.0078 | H | 28.0310 | $C_2H_4$ |
| 12.0000 | C | 30.9997 | $H_3Si$ |
| 13.0078 | CH | 40.0291 | $C_3H_4$ |
| 14.0157 | $CH_2$ | 42.0441 | $C_3H_6$ |
| 15.0246 | $CH_3$ | 50.0088 | $C_4H_2$ |
| 26.0150 | $C_2H_2$ | 51.0218 | $C_4H_3$ |
| 27.0238 | $C_2H_3$ | 65.0370 | $C_5H_5$ |
| 29.0405 | $C_2H_5$ | 67.0565 | $C_5H_7$ |
| 39.0229 | $C_3H_3$ | 77.0297 | $C_6H_5$ |
| 41.0404 | $C_3H_5$ | 79.0386 | $C_6H_7$ |
| 43.0576 | $C_3H_7$ | 81.0722 | $C_6H_9$ |
| 53.0390 | $C_4H_5$ | 83.0968 | $C_6H_{11}$ |
| 55.0567 | $C_4H_7$ | 85.1123 | $C_6H_{13}$ |
| 57.0739 | $C_4H_9$ | 91.0494 | $C_7H_7$ |
| 69.0719 | $C_5H_9$ | 93.0653 | $C_7H_9$ |
| 71.0929 | $C_5H_{11}$ | 95.0893 | $C_7H_{11}$ |
| 73.0751 | $C_4H_9O$ | 97.1010 | $C_7H_{13}$ |
| | | 113.0926 | $C_7H_{13}O$ |
| | | 147.0965 | $C_{10}H_{11}O$ |

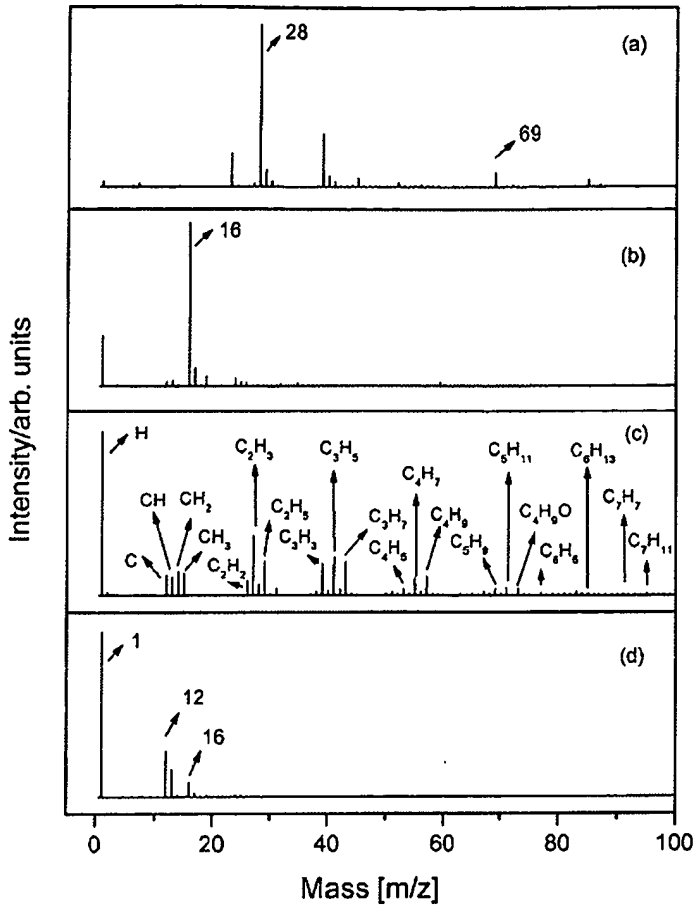


*Figure 2* ToF-SIMS characterization of the substrate and carbon film. (a) The positive ion ToF-SIMS spectrum ($m/e$ = 0–200) of a noncoated cleaned commercial silicon wafer. (b) The negative ion ToF-SIMS spectrum ($m/e$ = 0–200) of a noncoated cleaned commercial silicon wafer. (c) The positive ion ToF-SIMS spectrum ($m/e$ = 0–200) of a cleaned commercial silicon wafer coated with a hydrogenated carbon film that showed a large $H^+$ peak and hydrocarbon fragments $C_xH_y^+$ given in Table I. (d) The negative ion ToF-SIMS spectrum ($m/e$ = 0–200) of a cleaned commercial silicon wafer coated with a hydrogenated carbon film that was dominated by hydride ion ($H^-$) and carbon ion ($C^-$). Very little oxide ($O^-$) or hydroxide ($OH^-$) was observed.

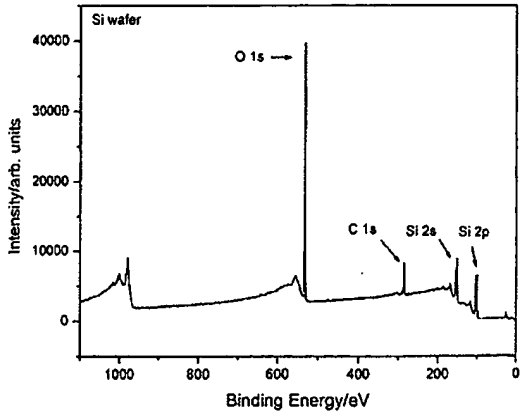


*Figure 3* The XPS survey scan of a cleaned commercial silicon wafer. Only silicon, oxygen, and trace carbon contamination were observed.

before and after being coated with a H*DLC film are shown in Figs 9 and 10 respectively. For comparison, a glassy carbon control spectrum is also shown in Fig. 10. The O 2*s* peak was observed in each case. In contrast to the glassy carbon and the untreated silicon wafer controls, a novel peak was observed at 49 eV in the XPS spectrum of the H*DLC film. This peak does not correspond to any of the primary elements carbon or oxygen shown in the survey scan in Fig. 4, wherein the peaks of these elements are given by Wagner *et al.* [33]. Hydrogen is the only element which does not have primary element peaks; thus, it is the only candidate to produce the novel peak and correspond to the surface H content of the H*DLC coatings. This peak closely matched and was assigned to a hydride given previously [29, 34–36].

## 3.3. Raman

The photomicrograph and the carbon Raman spectrum of the corresponding region of the H*DLC film are shown in Figs 11 and 12, respectively. The peak positions, full-width-half-maximum (FWHM), and peak areas were calculated by Gaussian curve fitting the baseline corrected spectrum. A broad band with a shoulder was observed at 1352.0 $cm^{-1}$, with a FWHM of 183 $cm^{-1}$, and a sharper feature was observed at

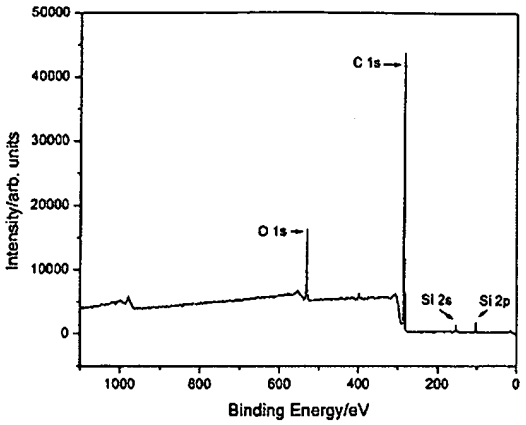


*Figure 4* The XPS survey scan of a cleaned commercial silicon wafer coated by reaction of a helium-hydrogen plasma with solid glassy carbon as the source of C. Only carbon and trace silicon and oxygen contamination were observed.

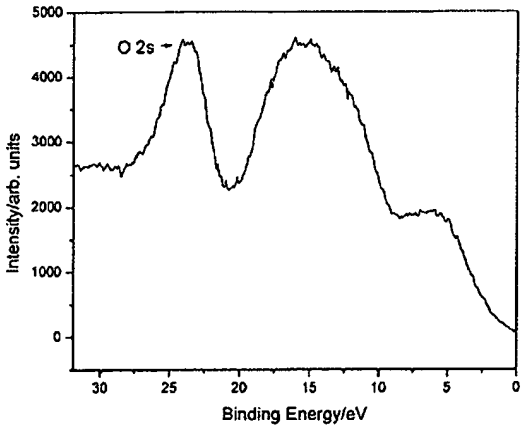


*Figure 6* High resolution XPS spectrum (0–35 eV) of the valence band region of a cleaned commercial silicon wafer coated with a hydrogenated carbon film that showed features that matched HDLC. An O 2s peak was also observed at 23 eV.

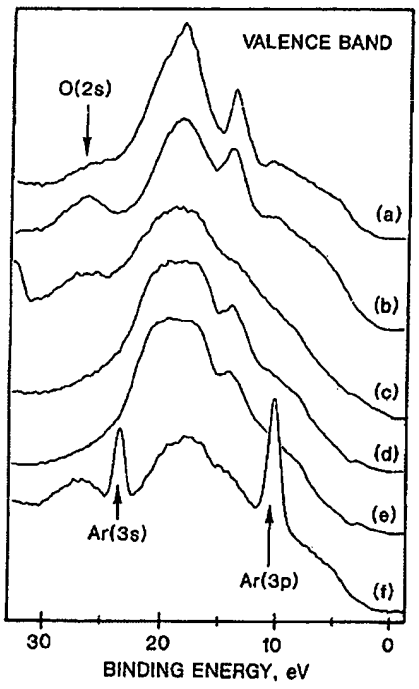


*Figure 5* High resolution XPS spectra (0–35 eV) of the valence band region of (a) single crystal diamond, (b) diamond film, (c) glassy carbon, (d) pyrolytic graphite, (e) mineral graphite, and (f) HDLC.

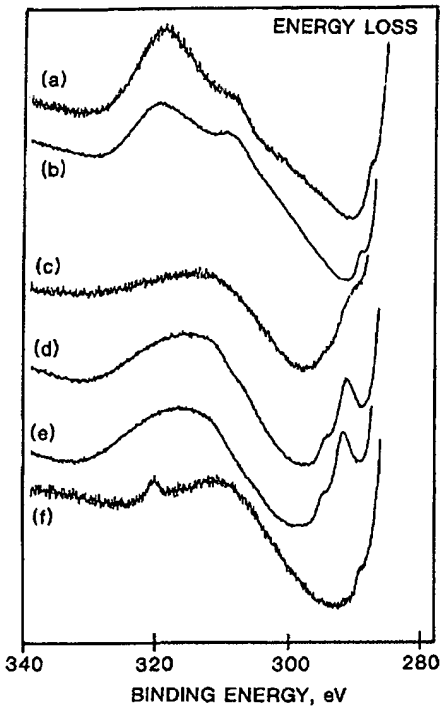


*Figure 7* High resolution XPS spectra (280–340 eV) of the C 1s energy loss region of (a) single crystal diamond, (b) diamond film, (c) glassy carbon, (d) pyrolytic graphite, (e) mineral graphite, and (f) HDLC.

1607.8 $cm^{-1}$ with a FWHM of 92 $cm^{-1}$. The position, peak shapes and separations matched that of HDLC [12]. Bands at 520 and 950 $cm^{-1}$ are the first and second order phonons of Si. The band at 2920 $cm^{-1}$ was assigned to an overtone of the G-band. The Raman spectrum confirmed the XPS results that the carbon film comprised H*DLC. Raman spectroscopy was also performed on the film from the quartz reactor wall. The results were similar to those of the H*DLC film on the silicon substrates.

### 3.4. Visible spectrum and line broadening

The Doppler-broadened line shape for atomic hydrogen has been studied on many sources such as hollow cathode [37, 38] and [39, 40] RF discharges. The energetic hydrogen atom densities and energies were calculated [26] from the intensities and widths of the 656.3 nm Balmer $\alpha$ line emitted from microwave discharge plasmas of $H_2$ compared with each of Xe-$H_2$ (90/10%) and He-$H_2$ (90/10%) as shown in Figs 13 and 14, respectively. The average He-$H_2$ Doppler

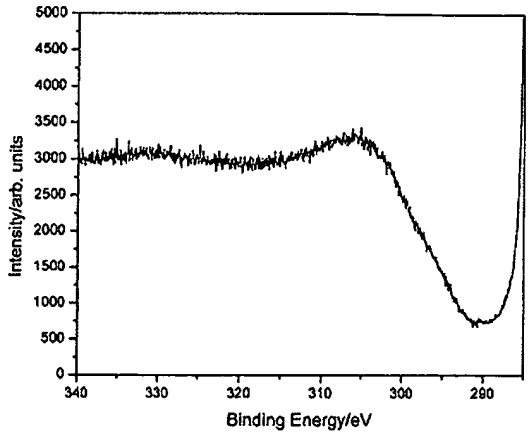


*Figure 8* High resolution XPS spectrum (280–340 eV) of the C1*s* energy loss region of a cleaned commercial silicon wafer coated with a hydrogenated carbon film that showed features that matched HDLC.

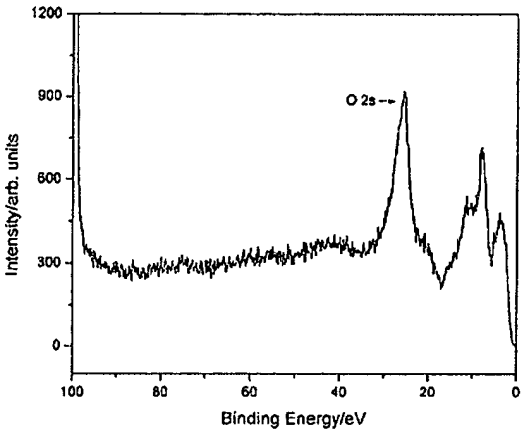


*Figure 9* The 0–100 eV binding energy region of a high resolution XPS spectrum of a cleaned commercial silicon wafer showing only a O2*s* peak in the low binding energy region.

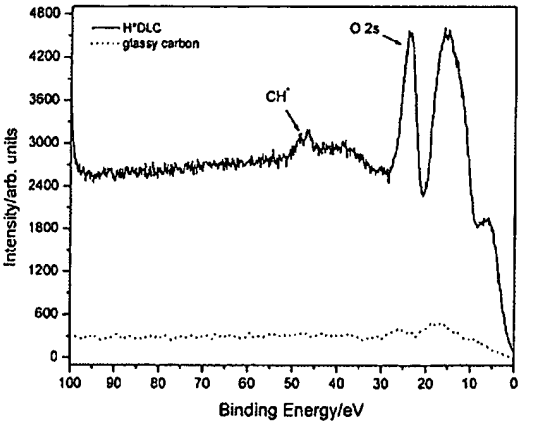


*Figure 10* The overlay of the 0–100 eV binding energy region of a high resolution XPS spectrum of glassy carbon (dotted line) and a cleaned commercial silicon wafer coated with a H*DLC film (solid line). A novel peak observed at 49 eV which could not be assigned to the elements identified by their primary XPS peaks was assigned to novel hydride CH*. The novel highly stable hydride formed by the catalytic reaction of $He^+$ and atomic hydrogen may be the basis of the novel method of formation of the H*DLC film.

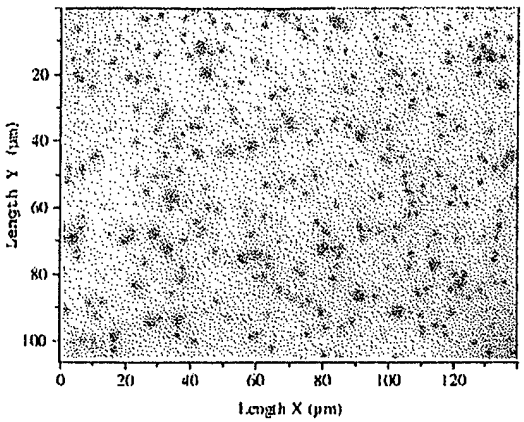


*Figure 11* The photomicrograph of a H*DLC film on a silicon wafer that was analyzed by Raman spectroscopy.

half-width was not appreciably changed with pressure. The corresponding energy of 180–210 eV and the number density of $5 \times 10^{11} \pm 20\%$ atoms/mm$^3$, depending on the pressure, were significant compared to only 2–3 eV and $7 \times 10^{10} \pm 20\%$ atoms/mm$^3$ for pure hydrogen, even though 10 times more hydrogen was present. Xe did not serve as a catalyst, and the plasma was much less energetic. Xe-$H_2$ showed no excessive broadening corresponding to an average hydrogen atom temperature of 2–3 eV, and the atom density was also low, $3 \times 10^{10} \pm 20\%$ atom/mm$^3$. Only the hydrogen lines were broadened. For example, the 667.816 nm He I line width was also recorded with the high resolution (±0.006 nm) visible spectrometer on He-$H_2$ (90/10%) and He microwave discharge plasmas as shown in Fig. 15. No broadening was observed in either case.

We have assumed that Doppler broadening due to thermal motion was the dominant source to the extent that other sources may be neglected. This assumption was confirmed when each source was considered. In general, the experimental profile is a convolution of a Doppler profile, an instrumental profile, the natural (lifetime) profile, Stark profiles, van der Waals profiles, a resonance profile, and fine structure. The electron density of the helium-hydrogen plasma recorded with a compensated Langmuir probe was about $n_e \sim 10^5$ mm$^{-3}$. This density was six to seven orders of magnitude too low for detectable Stark broadening, and the contribution from each remaining source was determined to be below the limit of detection [26].

## 4. Discussion

Silicon substrates were coated by the reaction product of a low power, low pressure He (90–70%)/$H_2$ (10–30%) microwave discharge plasma with glassy or graphitic carbon as the source of C. The ToF-SIMS identified the coatings as hydride by the large $H^+$ peak in the positive spectrum and the dominant $H^-$ in the negative spectrum. The XPS matched hydrogenated diamond-like carbon, and the H*DLC films was confirmed by features of the Raman peaks at 1352.0 and 1607.8 cm$^{-1}$. XPS further identified the surface H

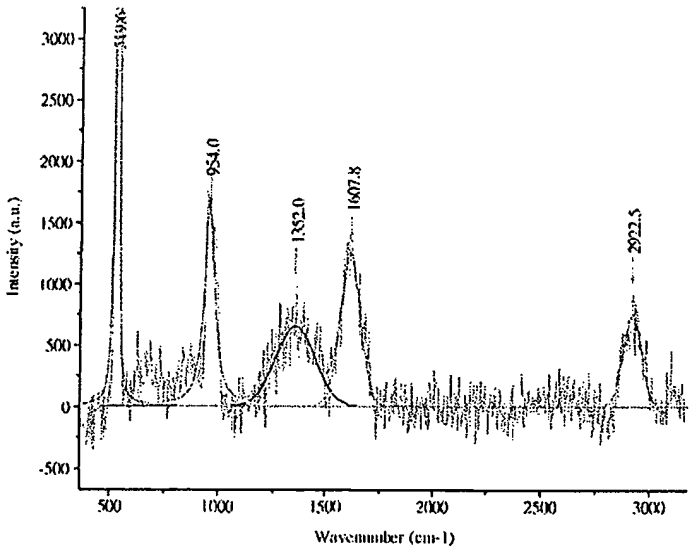


*Figure 12* The Raman spectrum recorded on the region shown in Fig. 11. A broad band with a shoulder was observed at 1352.0 $cm^{-1}$, with a FWHM of 183 $cm^{-1}$, and a sharper feature was observed at 1607.8 $cm^{-1}$ with a FWHM of 92 $cm^{-1}$. The position, peak shapes and separations matched that of DLC.

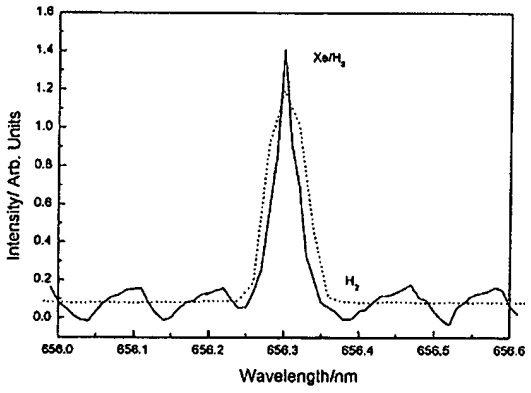


*Figure 13* The 656.3 nm Balmer $\alpha$ line width recorded with a high resolution (±0.006 nm) visible spectrometer on a xenon-hydrogen (90/10%) and a hydrogen microwave discharge plasma. No excessive line broadening was observed corresponding to an average hydrogen atom temperature of 3–4 eV.

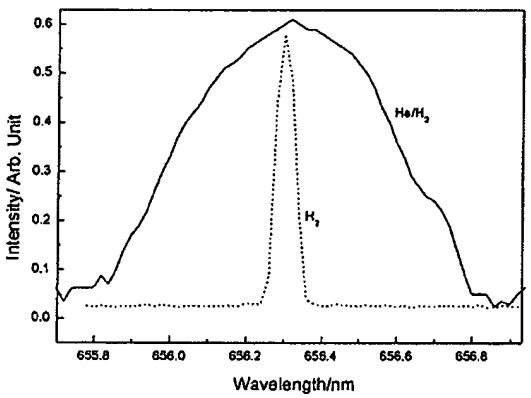


*Figure 14* The 656.3 nm Balmer $\alpha$ line width recorded with a high resolution (±0.006 nm) visible spectrometer on a helium-hydrogen (90/10%) and a hydrogen microwave discharge plasma. Significant broadening was observed corresponding to an average hydrogen atom temperature of 180–210 eV.

content of the H*DLC coatings as a novel hydride CH* corresponding to a peak predicted at 49 eV [29, 34–36]. The novel hydride is proposed to form by the catalytic reaction of $He^+$ with atomic hydrogen and subsequent autocatalytic reactions [27] to form highly stable carbon hydride products, H*DLC, comprising CH*. The novel highly stable hydride formed by the catalytic reaction of $He^+$ and atomic hydrogen and the energetic plasma itself having fast H may be the basis of a novel method of formation of the H*DLC film from solid carbon. We consider four possible mechanisms based on the unique conditions provided by the catalytic reaction.

It was observed that microwave He-$H_2$ plasmas showed extraordinary broadening corresponding to an average hydrogen atom temperature of 180–210 eV compared to $\approx$ 3 eV for plasmas of pure $H_2$ and Xe-$H_2$. The noble gas-hydrogen plasma that was energetic (He-$H_2$ plasma) formed DLC films when a solid carbon source, was present. The mechanism may be based on energetic hydrogen formed in the plasma reaction. Diamond and DLC are metastable materials; thus, continuous bombardment of the surface with energetic species that produce thermal and pressure spikes at the growth surface is required for deposition of diamond, DLC, and related films [41]. By quenching a beam of $C^+$ ions accelerated in an ultrahigh vacuum to a negatively biased substrate, Aisenberg and Chabot [13] were able to deposit DLC films for the first time. Rather than resulting in commercially useful processes, subsequently developed beam-type and sputtering production methods are essentially used for research. Exemplary methods discussed by Grill and Meyerson [42] are single low-energy beams of carbon ions, dual ion beams of carbon and argon, ion plating, RF sputtering or

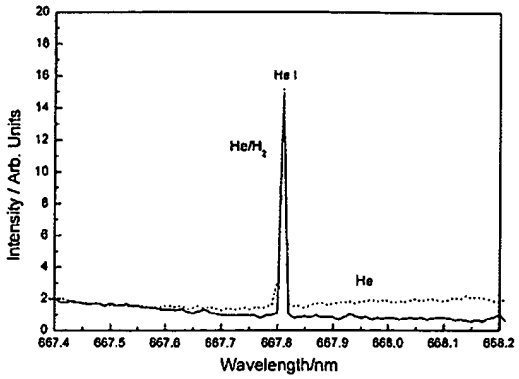


*Figure 15* The 667.816 nm He I line width recorded with a high resolution (±0.006 nm) visible spectrometer on helium-hydrogen (90/10%) (solid curve) and helium (dotted curve) microwave discharge plasmas. No broadening was observed in either case.

ion-beam sputtering from carbon/graphite targets, vacuum-arc discharges, and laser ablation. Using sputter deposition, amorphous DLC coatings can be prepared at low temperature due to energetic ion bombardment during the deposition of carbon. The absence of ion bombardment during carbon deposition leads to soft, conductive carbon films with no diamond-like properties. It has been shown that films with diamond-like properties are produced at ion energies of about 100 eV [9, 10]. Bombardment of the depositing carbon film by energetic H that produce a "thermal spike" has recently been confirmed [43] as the primary mechanism for the formation of diamond wherein the fast H was formed by charge acceleration in a high field. Here, an H atom-energy transfer to carbon atoms of a few 100 eV was found to be optimal for the transition of carbon films to diamond ($sp^3$-bonded carbon). Thus, the energetic species such as fast H formed in the helium-hydrogen microwave plasma may be the basis of the formation of the H*DLC film from solid carbon. In recent work [44] using hydrocarbon sources of carbon, this catalytic plasma reaction has shown the possibility for a significant advancement in the production of polycrystalline diamond as well.

The presence of hydrogen is an essential condition for the formation of DLC in many systems [12] by the stabilization of $sp^3$ carbon. The helium-hydrogen plasmas also form novel hydrides which may stabilize $sp^3$ carbon. Thus, a novel H intermediate formed by the plasma catalysis reaction may serve the stabilization role of H used in past systems.

The presence of novel hydride ions on the surface observed by XPS has implications that the mechanism of diamond-like carbon formation involves one or both of selective etching of graphitic carbon and the activation of surface carbon by the hydrogen catalysis product. Although the mechanism of diamond growth on a seed of diamond is still somewhat of a mystery, it is believed to be based on the extraction of H of a CH terminal bond to form a dangling carbon center to which $CH_3$ reacts. A carbon-carbon bond forms between adjacent methyl groups, and the hydrogen is gradually extracted, probably by H forming $H_2$. The further preferential degradation of graphitic carbon over diamond carbon by hydrogen permits diamond growth [45]. Thus, a novel H intermediate formed by the plasma catalysis reaction may serve the extraction role of H used in past systems that form diamond ($sp^3$ carbon).

Alternatively, the binding of novel H to graphitic carbon may cause a conversion to the diamond form. Novel EUV emission lines from microwave and glow discharges of helium with 2% hydrogen with energies of $q \cdot 13.6$ eV where $q = 1, 2, 3, 4, 6, 7, 8, 9, 11, 12$ or these lines inelastically scattered by helium atoms in the excitation of He ($1s^2$) to He ($1s^1 2p^1$) were identified as novel H ($1s^2$) intermediates [27, 28]. And, novel hydride compounds $MH^*$ and $MH_2^*$ wherein M is the alkali or alkaline earth metal and $H^*$ comprising a novel high binding energy hydride ions were identified previously [29, 34–36, 46] by a large distinct upfield resonance that showed that the hydride ion was different from the hydride ion of the corresponding known compound of the same composition [46]. The shift matched theoretical predictions [36]. Pronounced effects of dopants on the structure and properties of crystalline materials are well known [47, 48]. In the case of carbon, the binding of the novel H may thermodynamically favor $sp^3$ carbon over the graphitic form which could be the basis of a mechanism for the formation of DLC under our unique conditions.

## 5. Conclusion

Using a catalytic plasma reaction, it has been shown that solid carbon can be converted to H*DLC on silicon substrates using low power, mild conditions. The presence of novel hydride ions on the surface observed by XPS has implications that the mechanism of H*DLC formation involves one or more of stabilization of $sp^3$ carbon, selective etching of graphitic carbon, and the activation of surface carbon by the hydrogen catalysis product. Alternatively, H*DLC may form by the bombardment of CVD carbon by energetic hydrogen atoms formed in the catalytic plasma. Energetic species such as fast H formed in the helium-hydrogen microwave plasma that showed extraordinary Balmer $\alpha$ line broadening corresponding to an average hydrogen atom temperature of 180–210 eV may be the basis of the formation of the H*DLC film from solid carbon.

## Acknowledgments

Thanks to A. Miller of Lehigh University for XPS analysis and very useful discussions, and V. Pajcini of Charles Evans & Associates for Raman analysis and useful discussions.

## References

1. J. SETH, M. I. CHAUDHRY and S. V. BABU, *J. Vac. Sci. Technol.* **10** (1992) 3125.
2. G. F. ZHANG and X. ZHENG, *Surf. Coat. Technol.* **82** (1996) 110.
3. J. ROBERTSON, *Diamond Relat. Mater.* **1** (1992) 397.
4. S. AIESENBERG and F. M. KIMOCK, *Mater. Sci. Forum* **52/53** (1989) 1.

5. I. R. MCCOLL, T. L. PARKER and A. A. GORUPPA, *Diamond Relat. Mater.* 3 (1993) 83.
6. K. ZOLYNSKI, P. WITKOWSKI, A. KALUZNY, Z. HAS, P. NIEDZIELSKI and S. MITURA, *J. Chem. Vapor Dep.* 4 (1996) 232.
7. D. R. MCKENZIE, *Rep. Prog. Phys.* 59 (1996) 1611.
8. J. DENG and M. BRAUN, *Diamond Relat. Mater.* 4 (1995) 936.
9. J. ISHIKAWA, K. OGAWA, K. MIYATA and T. TAKAGI, *Nucl. Instrum. Methods* B 21 (1987) 205.
10. F. ROSSI and B. ANDRE, in Proc. IP AT 1991, Brussels, CEP Consultants, Edinburgh, UK (1991) p. 43.
11. S. PRAWER K. W. NUGENT, Y. LIFSHITZ, G. D. LEMPERT, E. GROSSMAN, J. KULIK, I. AVIGAL and R. KALISH, *Diamond Relat. Mater.* 5 (1996) 433.
12. Q. WEI and J. NARAYAN, *Int. Mater. Rev.* 45(3) (2000) 133.
13. S. AISENBERG and R. CHABOT, *J. Appl. Phys.* 42 (1971) 2953.
14. A. M. JONES, C. J. BEDELL, G. DEARNALEY, C. JOHNSTON and J. M. OWENS, *Diamond Relat. Mater.* 1 (1992) 416.
15. D. NIR, R. KALISH and G. LEVIN, *Thin Solid Films* 117 (1985) 125.
16. A. GRILL, B. MEYERSON, V. PATEL, J. REIMER and M. PETRICH, *J. Appl. Phys.* 61 (1987) 2874.
17. W. J. WU and M. H. HON, *Thin Solid Films* 307 (1997) 1.
18. O. MATSUMOTO, H. TOSHIMA and Y. KANZAKI, *ibid.* 128 (1985) 341.
19. B. H. LUNG, M. J. CHIANG and M. H. HON, *ibid.* 392 (2001) 16.
20. I. G. BROWN, *Ann. Rev. Mater. Sci.* 28 (1998) 243.
21. S. NEUVILLE and A. MATTHEWS, *MRS Bull.* 22(9) (1997) 22.
22. S. XU, B. K. TAY, H. S. TAN, L. ZHONG, Y. Q. TU, S. R. P. SILVA and W. I. MILNE, *J. Appl. Phys.* 79 (1996) 7243.
23. N. SAVVIDES and B. WINDOW, *J. Vac. Sci. Technol.* A 3 (1985) 2386.
24. J. KULIK, Y. LIFSHITZ, G. D. LEMPERT, J. W. RABALAIS and D. MARTON, *J. Appl. Phys.* 76 (1994) 5063.
25. J. KRISHNASWAMY, A. RENGAN, J. NARAYAN, K. VEDAM and C. J. MCHARGUE, *Appl. Phys. Lett.* 54 (1989) 2455.
26. R. L. MILLS, P. RAY, B. DHANDAPANI, R. M. MAYO and J. HE, *J. Appl. Phys.* 92 (2002) 7008.
27. R. L. MILLS, P. RAY, B. DHANDAPANI, M. NANSTEEL, X. CHEN and J. HE, *J Mol. Struct.* 643(1–3) (2002) 43.
28. R. L. MILLS and P. RAY, *J. Phys.* D 36 (2003) 1535.
29. R. L. MILLS, J. HE, P. RAY, B. DHANDAPANI and X. CHEN, *Int. J. Hydrogen Energy.* 28(12) (2003) 1401.
30. J. TADIC, I. JURANIC and G. K. MOORTGAT, *J. Photochem. Photobiol.* A 143 (2000) 169.
31. F. F. CHEN, "Electric Probes," in "Plasma Diagnostic Techniques," edited by R. H. Huddleston and S. L. Leonard (Academic Press, NY, 1965).
32. Provided by A. Miller, Zettlemoyer Center for Surface Studies, Sinclair Laboratory, Lehigh University, Bethlehem, PA.
33. C. D. WAGNER, W. M. RIGGS, L. E. DAVIS, J. F. MOULDER and G. E. MULILENBERG (eds.), in "Handbook of X-ray Photoelectron Spectroscopy" (Perkin-Elmer Corp., Eden Prairie, MN, 1997).
34. R. L. MILLS and P. RAY, *Int. J. Hydrogen Energy* 28 (2003) 825.
35. R. MILLS, B. DHANDAPANI, M. NANSTEEL, J. HE, T. SHANNON and A. ECHEZURIA, *ibid.* 26 (2001) 339.
36. R. MILLS, P. RAY, B. DHANDAPANI, W. GOOD, P. JANSSON, M. NANSTEEL, J. HE and A. VOIGT, *Eur. Phys. J., Appl. Phys.*, submitted.
37. I. R. VIDENOVIC, N. KONJEVIC and M. M. KURAICA, *Spectrochim. Acta*, Part B 51 (1996) 1707.
38. S. ALEXIOU and E. LEBOUCHER-DALIMIER, *Phys. Rev.* E 60 (1999) 3436.
39. S. DJUROVIC and J. R. ROBERTS, *J. Appl. Phys.* 74 (1993) 6558.
40. S. B. RADOVANOV, K. DZIERZEGA, J. R. ROBERTS and J. K. OLTHOFF, *Appl. Phys. Lett.* 66 (1995) 2637.
41. C. WEISSMANTEL, in "Thin Films from Free Atoms and Molecules," edited by K. J. Klabunde (Academic Press, Inc., New York, 1985) p. 153.
42. A. GRILL and B. MEYERSON, in "Synthetic Diamond: Emerging CVD Science and Technology," edited by K. E. Spear and J. P. Dismukes (John Wiley & Sons, Inc., New York, 1994) p. 91.
43. Y. LIFSHITZ, TH. KÖHLER, TH. FRAUENHEIM, I. GUZMANN, A. HOFFMAN, R. Q. ZHANG, X. T. ZHOU and S. T. LEE, *Science* 297 (2002) 1531.
44. R. L. MILLS, J. SANKAR, A. VOIGT, J. HE and B. DHANDAPANI, *Chem. Mater.* 15 (2003) 1313.
45. P. W. MAY, *Phil. Trans. R. Soc. Lond.* A 358 (2000) 473.
46. R. MILLS, B. DHANDAPANI, M. NANSTEEL, J. HE and A. VOIGT, *Int. J. Hydrogen Energy* 26 (2001) 965.
47. K. KIM, G. HONG, D. WON, B. KIM, H. MOON and D. SUHR, *J. Mater. Res.* 7 (1992) 2349.
48. M. C. MARTIN, G. SHIRANE, Y. ENDOH, K. HIROTA, Y. MORITOMO and Y. TOKURA, *Phys. Rev.* B 53 (1996) 14,285.

*Received 24 July 2003*
*and accepted 15 January 2004*